

Infrared Spectrum of the Protonated Water Dimer

Oriol Vendrell,¹ Fabien Gatti,² and Hans-Dieter Meyer^{1,*}

¹*Theoretische Chemie, Physikalisch-Chemisches Institut,*

Universitaet Heidelberg, Im Neuenheimer Feld 229, 69120 Heidelberg, Germany

²*LDSMS (UMR 536-CNRS), CC 014, Université de Montpellier II, F-34095 Montpellier, Cedex 05, France*

(Dated: January 17, 2007)

We report on a full quantum simulation of the infrared absorption spectrum of the protonated water dimer (H_5O_2^+) in the spectral range 0-4000 cm^{-1} . The doublet-peak feature around 1000 cm^{-1} , which was not understood and subject of debate, is reproduced, assigned and explained. Strong couplings between the proton-transfer and other modes are clearly identified, and their role in the spectrum is clarified. Low-frequency anharmonic torsions are discussed and described in detail for the first time.

PACS numbers: 33.20.Ea, 02.70.Ns, 31.15.Qg

Accurate infrared (IR) spectroscopy of protonated water clusters prepared in the gas phase has become possible in recent years [1, 2, 3, 4, 5], opening the door to a deeper understanding of the properties of aqueous systems, which are of main interest in central areas of chemistry and biology. Several computational studies have appeared in parallel, providing a necessary theoretical basis for the assignment and understanding of the different spectral features [5, 6, 7, 8, 9, 10]. The protonated water dimer (H_5O_2^+) is the smallest of the protonated water clusters, and it plays an important role in understanding the structure of the hydrated proton in water [11]. The IR spectroscopy of H_5O_2^+ remains an elusive problem, and some important features of its IR spectrum have not yet been conclusively assigned. In particular a double-peak structure near 1000 cm^{-1} had remained a mystery.

The IR predissociation spectrum of the H_5O_2^+ cation has been recently measured in argon-solvate [3] and neon- and argon-solvate [5] conditions. It is expected that the photodissociation spectrum of the $\text{H}_5\text{O}_2^+\cdot\text{Ne}_1$ complex is close to the linear absorption spectrum of the bare cation [5]. This spectrum features a doublet structure in the region of 1000 cm^{-1} made of two well-defined absorptions at 928 cm^{-1} and 1047 cm^{-1} . This doublet structure was not fully understood, although the highest-energy component was assigned to the asymmetric proton-stretch fundamental ($[\text{O}-\text{H}-\text{O}_{\parallel}]$) [5]. At the same time, recent classical-dynamics simulations on accurate potential energy surfaces (PES) have shown that the $[\text{O}-\text{H}-\text{O}_{\parallel}]$ motion features large amplitude displacements strongly coupled to other modes of the system [9, 10]. The best and most comprehensive quantal calculations on the IR spectrum of H_5O_2^+ so far are those of Bowman and coworkers [5]. Despite recent theoretical and experimental studies on this system, little is known about the lowest-frequency region, between 0 and 900 cm^{-1} . Modes vibrating in this frequency range are strongly anharmonic, and thus harmonic-vibrational-analysis results are of little value in shedding light on that matter. These low-frequency

modes may also play an important role in combination with the $[\text{O}-\text{H}-\text{O}_{\parallel}]$ fundamental. Such a possibility has been already suggested [2, 8, 9], but just which modes would participate in such combinations, and how, is still a matter of discussion.

In this letter we report the simulation of the IR linear absorption spectrum of the H_5O_2^+ cation in the range between 0 to 4000 cm^{-1} . For the first time the doublet-peak feature at around 1000 cm^{-1} is fully reproduced, analyzed and assigned. Predictions are also made for the lowest frequency part of the spectrum. Several important features of the system are analyzed for the first time, namely the degeneracy of some of the vibrational levels and the extreme anharmonicity of the wagging motions and relative internal rotation of the two water molecules. In doing so, we do not resort to any low-dimensional model of the system, but we treat it in its full dimensionality, which for a system of $N = 7$ atoms means $3N - 6 = 15$ active internal coordinates (15D). The use of full dimensionality is found crucial in the reproduction of the complete absorption spectrum. Our study provides a picture of the H_5O_2^+ system, extendable to larger aggregates, in which the clusters have to be viewed as highly anharmonic, flexible, multi-minima, coupled systems. We show that a full quantum-dynamical description of such a complex molecular system can still be achieved, providing explicative and predictive power and a very good agreement to available experimental data. In this respect, the reported simulations represent the state of the art in *quantum dynamically* describing an anharmonic, highly coupled molecular system of the size of the H_5O_2^+ cation. To account for the interatomic potential and the interaction with the radiation we make use of the potential energy surface (PES) and dipole-moment surfaces recently developed by Bowman and collaborators [6], which constitute the most accurate *ab initio* surfaces available to date for this system.

The quantum-dynamical problem is solved in the time-dependent picture using the multiconfiguration time dependent Hartree method (MCTDH)[12, 13]. MCTDH

is an efficient algorithm to solve the time-dependent Schrödinger equation by means of a variationally optimal multiconfigurational expansion of the wavefunction. Each configuration is given by a Hartree product of functions depending on a single or a group of degrees of freedom, the so-called single-particle functions (SPF). Both the multiconfigurational expansion coefficients and the SPF are allowed to vary simultaneously in time, which dramatically reduces the amount of configurations necessary to achieve a converged propagation as compared to the standard, numerically exact, propagation method. By controlling the number of configurations, MCTDH can be made as close to exact as desired, at the cost of an increased computational effort. The MCTDH program is also capable of using the time-independent picture, allowing for the convergence to eigenstates and eigenenergies of the Hamiltonian at hand. The algorithm that implements this feature is called *improved relaxation* [13, 14]. This algorithm is essentially a multiconfiguration self-consistent field approach that takes advantage of the MCTDH machinery. Several eigenenergies and eigenstates have been calculated using *improved relaxation*. They are invaluable in the assignments of some bands coming from the time-dependent calculation of the IR spectrum, and provide a total characterization of the corresponding states in terms of their fully-correlated wavefunctions. All the reported simulations were performed with the Heidelberg MCTDH package of programs [15].

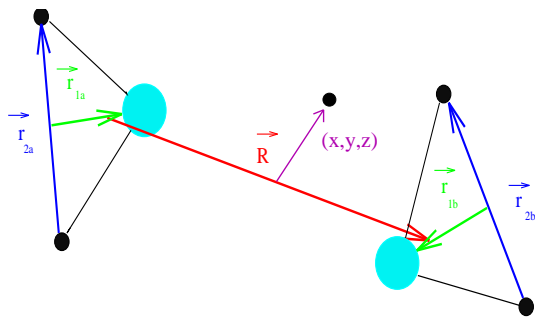


FIG. 1: (color online) Set of Jacobi vectors in terms of which the kinetic energy of the system is expressed. The set of internal coordinates used corresponds to the length of these vectors and relative angles.

The Hamiltonian of the system is expressed in a set of polyspherical coordinates based on Jacobi vectors [16]. It is found that only after the introduction of such a curvilinear set of coordinates an adequate treatment of the anharmonic large-amplitude vibrations and torsions of the molecule becomes possible. The kinetic energy operator is *exact* for $J = 0$, and the derivation of its lengthy formula (674 terms) will be discussed in a forthcoming publication. The correctness of the operator implemented was checked by comparison with data generated by the TNUM program [17]. The internal coordinates used are:

the distance between the centers of mass of both water molecules (R), the position of the central proton with respect to the center of mass of the water dimer (x, y, z), the Euler angles defining the relative orientation between the two water molecules (waggings: γ_a, γ_b ; rockings: β_a, β_b ; internal relative rotation: α) and the Jacobi coordinates which account for the particular configuration of each water molecule ($r_{1(a,b)}, r_{2(a,b)}, \theta_{(a,b)}$) where r_{1x} is the distance between the oxygen atom and the center of mass of the corresponding H_2 fragment, r_{2x} is the H–H distance and θ_x is the angle between these two vectors. These coordinates have the great advantage of leading to a much more decoupled representation of the PES than a normal-mode based Hamiltonian.

As outlined above, the wavefunction is represented by products of SPFs which in turn are represented by discrete variable representation (DVR) grids. The total primitive product-grid consists of 1.3×10^{15} points. This number makes clear that the potential must be represented in a more compact form to make calculations feasible. We choose to represent the PES as follows: the coordinates are divided in five groups, $\mathbf{g}_1 \equiv [x, y, z, \alpha]$, $\mathbf{g}_2 \equiv [\gamma_a, \gamma_b]$, $\mathbf{g}_3 \equiv [R, \beta_a, \beta_b]$, $\mathbf{g}_4 \equiv [r_{1a}, r_{2a}, \theta_a]$ and $\mathbf{g}_5 \equiv [r_{1b}, r_{2b}, \theta_b]$. The potential is then expanded as [18]:

$$\hat{V}(\mathbf{c}) = \hat{v}^{(0)} + \sum_{i=1}^5 \hat{v}_i^{(1)}(\mathbf{g}_i) + \sum_{i=1}^4 \sum_{j=i+1}^5 \hat{v}_{ij}^{(2)}(\mathbf{g}_i, \mathbf{g}_j) + \hat{v}_{z,2,3}^{(3)}(z, \mathbf{g}_2, \mathbf{g}_3) \quad (1)$$

where $\mathbf{c} \equiv [\mathbf{g}_1, \dots, \mathbf{g}_5]$. The $\hat{v}^{(0)}$ term is the energy at the reference geometry. The $\hat{v}_i^{(1)}$ terms are the intra-group potentials obtained by keeping the coordinates in other groups at the reference geometry, while the $\hat{v}_{ij}^{(2)}$ terms account for the group-group correlations. The potential with up to second-order terms gives already a very reasonable description of the system. The $\hat{v}_{z,2,3}^{(3)}$ term accounts for three-mode correlations between the displacement of the central proton, the distance between both water molecules and the angular wagging and rocking motions. This PES representation may be sequentially improved in a convergent series by adding more correction terms where coordinates belonging to three or more different groups are allowed to vary simultaneously. However, the PES in Eq. 1 is found to reproduce the full potential very well, providing a converged zero-point energy of 12376.3 cm^{-1} , 16 cm^{-1} below the reported Diffusion-Monte-Carlo result [19] on the full potential.

In Fig. 2 the probability-density projection on the wagging coordinates is shown for the ground vibrational state (g_0), as well as for one of the two fundamental states (w_{1a}, w_{1b}) of the wagging modes, which are degenerate vibrational states with an energy of 106 cm^{-1} . The energies of the next three wagging-mode states (w_2, w_3, w_4) are, respectively, 232 , 374 and 422 cm^{-1} . State w_3 is

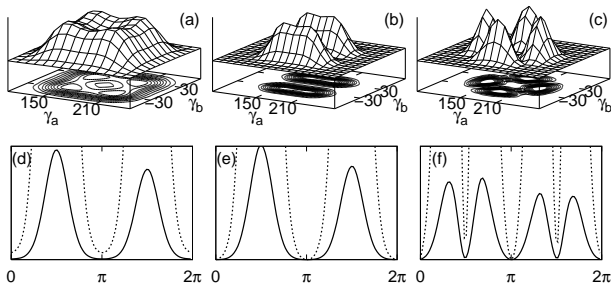


FIG. 2: Probability density of the ground vibrational state (a), first (b) and third (c) wagging-mode states projected onto the wagging coordinates γ_a and γ_b . Ground vibrational state (d), splitting state (e) and second excited internal-rotation state (f) projected onto the α coordinate. An extended scale ($\times 10$) is used to clarify existence and position of nodes.

shown in Fig. 2c. State w_2 has an energy that nearly doubles the energy of the w_{1x} states, since it has been seen to roughly correspond to one quantum in state w_{1a} and one quantum in state w_{1b} . The strong anharmonicity of the wagging motions can be further appreciated in the progression of w_2 , w_3 and w_4 vibrational-state energies. In addition, the harmonic-analysis energies of the two lowest wagging-fundamentals w_{1a} and w_{1b} are around 300 cm^{-1} larger than the MCTDH result and do not account for their degeneracy, since harmonic modes are constructed taking as a reference the C_{2v} absolute minimum. The system, however, interconverts between equivalent C_{2v} minima and other stationary points through low-energy barriers (wagging motions and internal rotation), which leads to a highly symmetric ground-state wavefunction. The vibrational levels of H_5O_2^+ can be labeled according to the symmetry group \mathcal{G}_{16} , which is related to the \mathcal{D}_{2d} point group but with allowed permutation of the H-atoms within each of the two monomers [20]. The two lowest excited wagging/rocking modes transform according to an E representation within this symmetry group.

The first two excited states associated to the internal rotation ($g_0^{(-)}$, i_1) have energies of 1 and 160 cm^{-1} , respectively. Here $g_0^{(-)}$ is the splitting state whose probability density along α is shown in Fig. 2e, while the probability density for i_1 is shown in Fig. 2f. The first two fundamentals of the symmetric stretch ($[\text{O-O}]$, R coordinate) have energies of 550 and 1069 cm^{-1} respectively, while the rocking fundamentals, which are degenerate, have an energy of 456 cm^{-1} .

Figure 3 presents the IR predissociation spectrum of the $\text{H}_5\text{O}_2^+\cdot\text{Ne}$ complex [5] and the MCTDH spectrum of H_5O_2^+ in the range 700 - 1900 cm^{-1} . The MCTDH spectrum is obtained in the time-dependent picture by Fourier transformation of the autocorrelation of the

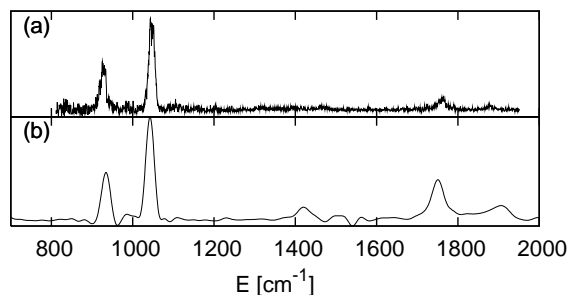


FIG. 3: Predissociation spectrum of the $\text{H}_5\text{O}_2^+\cdot\text{Ne}$ complex [5] (top) and MCTDH (bottom).

dipole-operated initial state [21]:

$$I(E) = \frac{E}{6 c \epsilon_0 \hbar^2} \int_{-\infty}^{\infty} \exp(i(E + E_0)t/\hbar) \times \langle \Psi_{\mu,0} | \exp(-i\hat{H}t/\hbar) | \Psi_{\mu,0} \rangle dt \quad (2)$$

where E_0 is the ground-state energy and $|\Psi_{\mu,0}\rangle \equiv \hat{\mu}|\Psi_0\rangle$. The MCTDH spectrum shows a good agreement with the experimental spectrum. The agreement on the doublet structure around 1000 cm^{-1} is very good, and the position of the doublet at 1700 - 1800 cm^{-1} is also in good agreement, despite the relative intensities being larger in MCTDH. The doublet absorption at around 1000 cm^{-1} deserves a deeper analysis. Due to the high density of states, it was not possible, by means of *improved relaxation*, to obtain the fully converged states, but reasonably good approximations to the wavefunctions of the low-energy ($|\Psi_d^l\rangle$, 930 cm^{-1}) and high energy ($|\Psi_d^h\rangle$, 1021 cm^{-1}) eigenstates of the doublet were computed. Even though these wavefunctions contain all the possible information on the two states, their direct analysis becomes complex due to the high dimensionality of such objects. In order to obtain a fundamental understanding of the observed bands, zeroth-order states were constructed by operating with \hat{z} on the ground state: $|\Phi_z\rangle = \hat{z}|\Psi_0\rangle N$, where N is a normalization constant, and by operating with $(\hat{R} - R_0)$ on the third excited wagging state w_3 : $|\Phi_{R,w_3}\rangle = (\hat{R} - R_0)|\Psi_{w_3}\rangle N$. The two eigenstates corresponding to the doublet were then projected onto these zeroth-order states. Note that $|\Phi_z\rangle$ is characterized by one quantum of excitation in the proton-transfer coordinate whereas $|\Phi_{R,w_3}\rangle$ by one quantum in $[\text{O-O}]$ and three quanta in the wagging motion. The corresponding overlaps read: $|\langle \Phi_z | \Psi_d^l \rangle|^2 = 0.20$, $|\langle \Phi_{R,w_3} | \Psi_d^l \rangle|^2 = 0.53$ and $|\langle \Phi_z | \Psi_d^h \rangle|^2 = 0.48$, $|\langle \Phi_{R,w_3} | \Psi_d^h \rangle|^2 = 0.12$. One should take into account that these numbers depend on the exact definition of the zeroth-order states, which is not unique. Also, the zeroth-order states do not span the same space as the two eigenstates, so the overlaps do not add up to 1. However, they provide a clear picture of the nature of the doublet: the low-energy band has the largest contribution from the combination of the symmetric stretch and

the third excited wagging (see Fig. 2), whereas the second largest is the proton-transfer motion. For the high-energy band the importance of these two contributions is reversed. Thus, the doublet may be regarded as a Fermi resonance between two zero-order states which are characterized by $(1R, 3w)$ and $(1z)$ excitations, respectively. The reason why the third wagging excitation plays an important role in the proton-transfer doublet is understood by inspecting Fig. 2c. The probability density of this state has four maxima, each of which corresponds to a planar conformation of $\text{H}_2\text{O}-\text{H}^+$ (H_3O^+ character) for one of the waters, and a bend conformation (H_2O character) where a lone-pair H_2O orbital forms a hydrogen bond with the central proton. When the proton oscillates between the two waters, the two conformations exchange their characters accordingly.

The simulated spectrum in the range between 0 and 4000 cm^{-1} is depicted in Fig. 4. The region below 700 cm^{-1} has not yet been accessed experimentally. Direct absorption of the wagging motions, excited by the perpendicular components of the dipole operator, appears in the range between $100 - 200\text{ cm}^{-1}$. The doublet starting at 1700 cm^{-1} is clearly related to bending motions of the water molecules, but its exact nature is still to be addressed. The MCTDH spectrum also shows the absorptions of the OH stretchings starting at 3600 cm^{-1} .

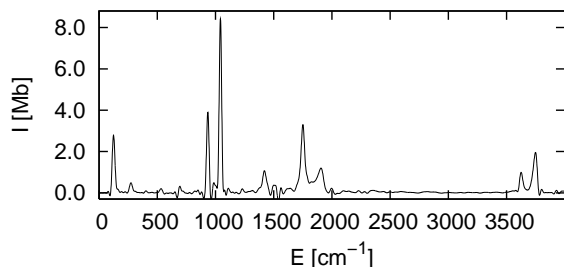


FIG. 4: Simulated MCTDH spectrum in the range between 0 and 4000 cm^{-1} . Absorption is given in absolute scale in mega-barns (Mb).

In conclusion, we report the simulation of the IR absorption spectrum of the H_5O_2^+ cation by means of quantum-dynamical methodology in the full spectral range between $0-4000\text{ cm}^{-1}$. The spectrum is directly comparable to available and future experiments on this system. We discuss some important features of the protonated water dimer which have remained until now elusive due to strongly anharmonic, large-amplitude motions. In particular, the doublet band absorption around 1000 cm^{-1} is fully reproduced and explained in terms of cou-

pling of the proton-transfer motion to wagging torsions of the water moieties. Other features of the system are discussed for the first time, namely the degeneracy of some of the vibrational levels, the splitting of vibrational levels arising from the internal rotation and the extreme anharmonicity of the wagging motions. Predictions are made for the low energy part of the spectrum. These calculations thus provide important fundamental information on the spectroscopy and dynamics of protonated aqueous systems.

The authors thank Prof. J. Bowman for providing the potential-energy routine, D. Lauvergnat for performing the TNUM calculations and the Scientific Supercomputing Center Karlsruhe for generously providing computer time. O. V. is grateful to the Alexander von Humboldt Foundation for financial support.

* Hans-Dieter.Meyer@pci.uni-heidelberg.de

- [1] K. R. Asmis, *et al.*, *Science* **299**, 1375 (2003).
- [2] T. D. Fridgen, *et al.*, *J. Phys. Chem. A* **108**, 9008 (2004).
- [3] J. M. Headrick, J. C. Bopp, and M. A. Johnson, *J. Chem. Phys.* **121**, 11523 (2004).
- [4] J. M. Headrick, *et al.*, *Science* **308**, 1765 (2005).
- [5] N. I. Hammer, *et al.*, *J. Chem. Phys.* **122**, 244301 (2005).
- [6] X. Huang, B. J. Braams, and J. M. Bowman, *J. Chem. Phys.* **122**, 044308 (2005).
- [7] M. V. Vener, O. Kühn, and J. Sauer, *J. Chem. Phys.* **114**, 240 (2001).
- [8] J. Dai, *et al.*, *J. Chem. Phys.* **119**, 6571 (2003).
- [9] J. Sauer and J. Dobler, *Chem. Phys. Chem.* **6**, 1706 (2005).
- [10] M. Kaledin, A. L. Kaledin, and J. M. Bowman, *J. Phys. Chem. A* **110**, 2933 (2006).
- [11] D. Marx, M. Tuckerman, J. Hutter, and M. Parrinello, *Nature* **397**, 601 (1999).
- [12] M. H. Beck, A. Jäckle, G. A. Worth, and H.-D. Meyer, *Phys. Rep.* **324**, 1 (2000).
- [13] H.-D. Meyer and G. A. Worth, *Theor. Chem. Acc.* **109**, 251 (2003).
- [14] H.-D. Meyer, F. L. Quéré, C. Léonard, and F. Gatti, *Chem. Phys.* **329**, 179 (2006).
- [15] G. A. Worth, M. H. Beck, A. Jäckle, and H.-D. Meyer, *The MCTDH Package, Version 8.4*, (2007). See <http://www.pci.uni-heidelberg.de/tc/usr/mctdh/>.
- [16] F. Gatti, *J. Chem. Phys.* **111**, 7225 (1999).
- [17] D. Lauvergnat and A. Nauts, *J. Chem. Phys.* **116**, 8560 (2002).
- [18] J. M. Bowman, S. Carter, and X. Huang, *Int. Rev. Phys. Chem.* **22**, 533 (2003).
- [19] A. B. McCoy, *et al.*, *J. Chem. Phys.* **122**, 061101 (2005).
- [20] D. J. Wales, *J. Chem. Phys.* **110**, 10403 (1999).
- [21] G. G. Balint-Kurti, R. N. Dixon, and C. C. Marston, *J. Chem. Soc., Faraday Trans.* **86**, 1741 (1990).